Journal of the Korean Physical Society, Vol. 72, No. 7, April 2018, pp. 818∼825

Measurement of Characteristic of X-band RF Cavity for 6 MeV Electron Linac

Seung-wook Shin, Seung-Hyun Lee and Seyoung Oh
Department of Energy Science, Sungkyunkwan University, Suwon 16419, Korea

Donghyup Ha, Mitra Ghergherehchi and Jongseo Chai*
College of Information & Communication Engineering, Sungkyunkwan University, Suwon 16419, Korea

Byung-no Lee and Moonsik Chae
Radiation Equipment Research Division, Korea Atomic Energy Research Institute, Advance Radiation Technology Institute, Jeongeup 34057, Korea

(Received 8 February 2018, in final form 2 March 2018)

A compact 6 MeV electron linear accelerator (linac), intended to be used as an X-ray source for a dual-head gantry radiotherapy system has been developed. In order to meet the size requirements of the dual-head gantry machine, an X-band radio frequency (RF) technology is used, which facilitates a reduction in the size of the linac, which is nine times smaller than the conventional medical purpose linac using S-band RF technology. Nevertheless, the X-band RF technology requires much higher machining precision and higher-quality surface finish owing to the electrical breakdown phenomena resulting from its small size. After the design was completed, the RF cavity was machined using high-precision machining technology, achieving machining tolerances of ±2 μm, and a surface roughness less than 50 nm. Various RF properties were measured in the fabricated RF cavity by using a network analyzer, and the distribution of the electric field generated in the RF cavity was verified by a bead-pull measurement technique. RF conditioning and beam commissioning experiments were performed, following the fabrication and tuning of the RF cavity.

PACS numbers: 87.56.bd, 29.20.Ej
Keywords: X-band, Electron linac, RF cavity
DOI: 10.3938/jkps.72.818

I. INTRODUCTION

The primary methods for treating cancer include surgical intervention, chemotherapy, and radiation therapy. Following the discovery of X-rays by Röntgen in 1895 and Radium in 1898 by Pierre and Marie Curie, direct radiation has been widely applied to cancer treatments with much success. In this regard, radiation therapy has contributed considerably to the development of treatment protocols in oncology during the 20th century. Cobalt radiotherapy was developed in 1951 followed by linear accelerator radiotherapy devices in 1952, as clinical tools for the effective treatment of deep tumors using high energy X-ray. These techniques facilitate the application of radiation therapy to more types of cancer [1]. Recently, a variety of radiation therapy devices have been developed that can destroy cancer cells without significant damage to healthy surrounding tissue. These include intensity-modulated radiotherapy (IMRT), image-guided radiotherapy (IGRT), and respiratory-gated radiotherapy (RGRT) [2].

Radiation therapy is a treatment protocol which uses ionized particles (protons, heavy ions, electrons) or photons (gamma rays or X-rays) to directly damage and destroy cancer cells. The particles used in this protocol are accelerated to high energies using particle accelerators such as linear accelerators, synchrotrons, and cyclotron, *etc.* However, the treatment procedure usually results in damage to normal healthy cells, in addition to cancer cells. Minimizing unwanted damage to cells is an important problem in the treatment of cancer and several strategies have been investigated, including the reduction of radiation exposure.

Sungkyunkwan University has developed a dual head gantry system since 2012, which is a radiation treatment system that reduces the amount of radiation exposure [3]. This system is characterized by the use of two electron linear accelerators to reduce the exposure time of patients by reducing the treatment time.

In radiotherapy, electron linear accelerators (linacs)

*E-mail: jschai@skku.edu

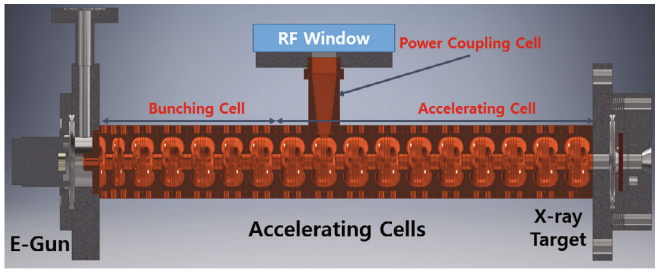

Fig. 1. (Color online) Structural figure of the Entire Electron Linac.

generally act as X-ray generators and accelerate electrons to several MeV depending on the treatment application. For clinical use, these devices use operating frequencies including the S-band (2.856 GHz) [4], C-band (6 GHz) [5], and X-band (9.3 GHz) [6,7] depending on the application. The higher the frequency band used, the shorter the wavelength, which facilitates a smaller footprint and ease of configuration. Since linac systems are typically bulky and the developmental cost can be high, the system under consideration exploits a frequency of 9.3 GHz in the X-band.

Owing to a wide variety of factors such as machining tolerance, brazing tolerance and surface roughness that are critical aspects during the fabrication process of an accelerator, there is always a difference between the design and the final product. Therefore, it is necessary to measure the characteristics of the radio frequency (RF) cavity such as the resonance frequency and the electric field distribution, prior to tuning. In this paper, we will focus on RF cavity testing, tuning, RF conditioning, and beam commissioning of a side-coupled standing-wave-type RF cavity with a resonance frequency of 9.3 GHz, with 6 MeV accelerated electrons.

II. SPECIFICATION OF 6 MEV X-BAND ELECTRON LINAC

The electron linac for the dual-head gantry radiotherapy machine consists of 17 cells in total. The 17 cells consist of 7 bunching cells, 9 accelerating cells, and one power coupler cell. The 1st bunching cell and 17th cell were modified to connect with the beam pipe. The E-gun for electron generation is coupled to the 1st bunching cell and there is a port for the vacuum pump in between. In 7 bunching cells, cell lengths were determined incident electrons to be bunched efficiently, accelerated efficiently to 1 MeV. The overall structure is shown in Fig. 1. By reducing a gap between nose-cone, we can achieve increment of the shunt impedance which leads to increment of an acceleration efficiency in accelerating cell. However, if the gap between the nose-cones is too narrow, the a electric field inside the cell will become too high and electrical breakdown may occur. Therefore, cells should be designed according to the voltage that does not cause electrical breakdown. In the 1950s, Kilpatric studied the relationship between electrical breakdown and resonant frequency when a RF signal was applied to a metal structure under vacuum conditions. RF cavities were designed based on the limit proposed by Kilpatric. The Kilpatric limit at an operating frequency 9.3 GHz is 79.37 MV/m. However, the presented RF cavity has a significantly improved vacuum state and surface roughness compared to those of the 1950s, so the Kilpatric's criterion value is scaled by multiplying the brave factor to give a value of 1.5 - 2. The peak value of the electric field of the proposed RF cavity is 86.6 MV/m, which is 1.09 times higher than that of the Kilpatric's criterion value. Experimental results of the X-band RF cavity from various institutes show that a peak electric field value of more than 300 MV/m can be generated [8–10]. Therefore, an electric field of 86.6 MV/m is in the safe range taking electrical breakdown into account. In addition, if the gap between the nose-cones is narrowed, dissipation power increases inside the cell, so it is important to find an optimal value. The effective shunt impedance value designed for effective electron beam acceleration of the accelerating cell is 105 MΩ/m. A preliminary study on the design of the electron linac for the dual-head gantry radiotherapy machine can be found in [11]. The detailed specification of the electron accelerator is shown in the Table 1.

Table 1. Specification of The 6 MeV Electron Linac.

Parameters	Value
Operating Frequency	9.3 GHz
Input RF power (pulsed)	< 2 MW
Pulse Length	4 us
Duty Factor	0.0018
E-gun Volage	15 kV
Output Beam Current (Pulsed Maximum)	30 mA
Average Beam Current	55 uA
Beam Spot Size (FWHM)	2 mm
Output Beam Energy	6 MeV
Effective Shunt Impedance per Unit Length	90 MΩ/m
Operating Mode	Standing Wave, Pi/2 mode
Structure Type	Side-coupled Cavity
Structure Aperture Radius	4 mm
Length of the Accelerating Structure	< 30 cm

A mechanical design process is required for the fabrication of accelerators as actual products. For stable accelerator operation, a constant temperature needs to be maintained in the accelerator. For temperature control, a cooling line is created, in which water passes through

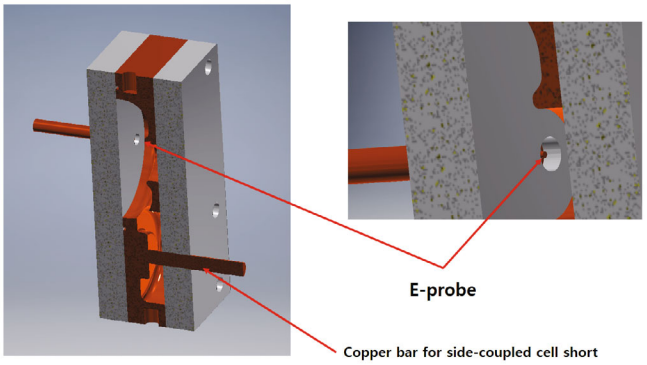

(a) normal cell

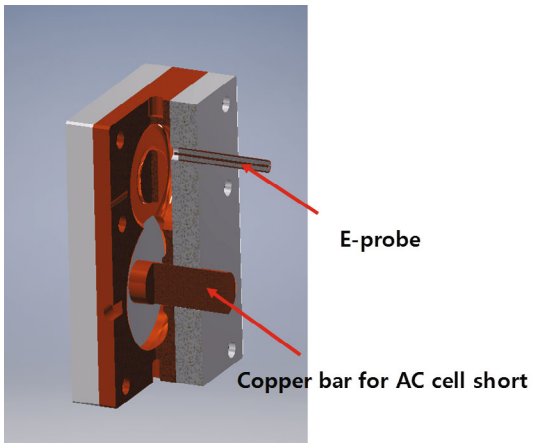

(b) side-coupled cell

Fig. 2. (Color online) Assembly of the RF cavity, jig, E-probe, and copper short-bar.

the accelerator. As manufacturing all parts of the accelerator at once is not possible, individual pieces were manufactured separately and then brazed together. Grooves were designed to ensure the flow of the brazing filler. Due to the thermal expansion of the brazing filler, the filler can flow into the RF cavity, which reduces the volume of the RF cavity and increases the resonance frequency of the entire accelerator. Stainless steel flanges were used to connect the assemblies of the E-gun and the beginning of the tungsten target and end position of the RF cavity.

III. RF PROPERTIES OF THE RF CAVITY AND RESULTS OF THE MEASUREMENT

It is important to confirm that the high-quality of surface roughness and tolerances, the operating frequency of the accelerator, and the shape of the electric field distribution in the accelerator are the same as the design specifications. If the operating frequency and field distribution in the accelerating tube differ from the design specifications, they can be reprocessed or mechanically

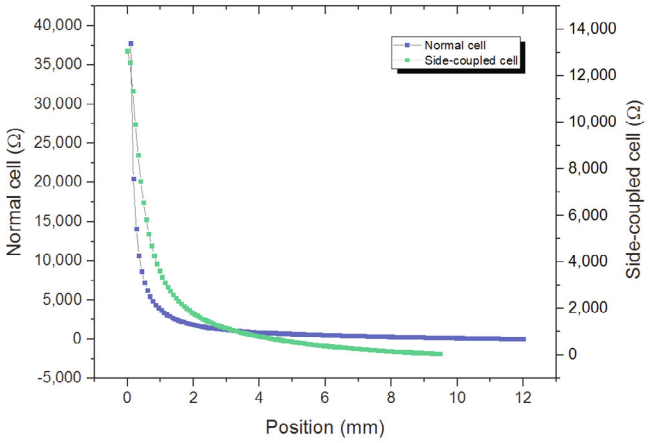

Fig. 3. (Color online) E_0/H_0 rations of normal and side-coupled cells.

tuned. In this section, the measurement and tuning of the RF properties of the RF cavity are discussed.

1. Measurement and Tuning of the Resonance Frequency

In order to measure the resonance frequency of the fabricated RF cavity, the RF cavity was mounted on a jig to create the same conditions as those of the simulation. After the RF cavity was assembled with the jig, the generated S11 signal was measured when the electrical probe was inserted into the RF cavity. The RF cavity mounted on the jig is shown in Fig. 2. A copper short-bar was used to create a condition without a generated electric field in the cell connected to the cell where the measurement is performed. As the electrical probe penetrates, it generates an additional impedance term in the RF cavity, thus the resonance frequency of the RF cavity changes according to the penetration depth. The energy generated inside the accelerating tube is affected by the additional perturbed component, where the energy change results in a change in the resonant frequency. Therefore the position where the frequency does not change when the electrical probe penetrates has to be located, thus the insertion position of the probe has to be determined.

In the 1950s, Slater [12] described the change in the resonance frequency with the change of the volume of the RF cavity. The Slater perturbation theorem can be expressed by the following equations:

$$\frac{\omega-\omega_0}{\omega_0}=\frac{\int_{\Delta v}[\mu|H_0|^2-\epsilon|E_0|^2]d\tau}{\int_v[\mu|H_0|^2+\epsilon|E_0|^2]d\tau}=\frac{\Delta U_m-\Delta U_e}{U} \quad (1)$$

with $U=\frac{1}{4}\int(\mu_0|H_0|^2+\epsilon_0|E_0|^2)dV$.

$$\Delta\omega=0\Rightarrow\frac{E_0}{H_0}=\sqrt{\mu_0/\epsilon_0}=377\ \Omega, \quad (2)$$

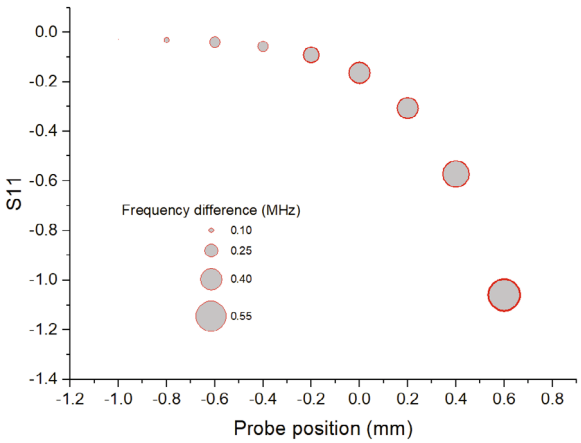

Fig. 4. (Color online) Change of S11 value according to depth of probe insertion.

Table 2. Simulation results of the resonance frequency of the RF cavity (all units are in GHz).

	Normal cell	Side-coupled cell
1^{st} bunching cell	9.2003	9.8071
2^{nd} bunching cell	9.2624	9.28496
3^{rd} bunching cell	9.2776	9.33462
4^{th} bunching cell	9.27948	9.31614
5^{th} bunching cell	9.27818	9.31008
6^{th} bunching cell	9.27652	9.30826
7^{th} bunching cell	9.27894	9.30286
Normal accelerating cell	9.2799	9.3058
Power coupler cell	9.2839	9.3424
End cell	9.25156	9.28798

(a)Measurement sample.

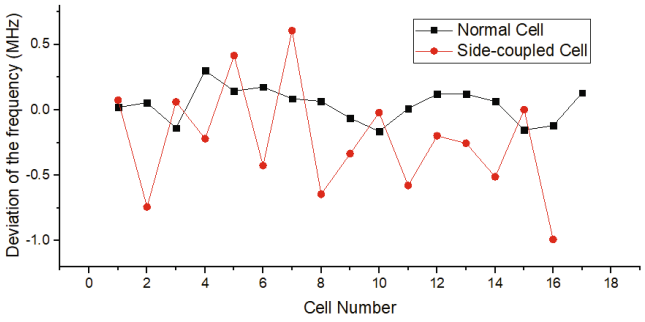

(b)Deviation of the frequency from the reference value.

Fig. 5. (Color online) Measurements of the resonance frequency of the RF cavity

where ω is the perturbed frequency, ω_0 is the unperturbed frequency, μ is the relative permeability, ϵ is the relative permittivity of material, H_0 is the unperturbed magnetic field, E_0 is the unperturbed electric field, U is the energy stored inside the RF cavity, ΔU_m and ΔU_e are time averaged magnetic and electric energies stored inside of the RF cavity, respectively.

The position where the change in the resonance frequency is minimized even with the additional perturbation term can be found by using Eq. (2). The location where the ratio of the electric and the magnetic fields generated in the RF cavity is 377 Ω is the position where the change of the resonance frequency can be minimized with the added perturbation term. Thus, the minimized resonance frequency of the RF cavity can be measured by inserting the probe at the position determined by the procedure above. The functions for E_0/H_0 in normal and side-coupled cells are shown in Fig. 3. The calculated position of $E_0/H_0 = 377\ \Omega$ is located 7.3 mm and 6.17 mm from the center of the cell for the normal cell and for the side-coupled cell, respectively. The previously calculated position represents the point at which the change in volume is the smallest. However, due to the volume of the electrical probe, the resonance frequency of the RF cavity changes when the probe is inserted. While the S11 value can be confirmed by receiving a proper signal at the time of inserting the probe, the change in resonance frequency needs to be very small. Figure 4 shows the variation in frequency with the insertion depth of the probe. The minimum value of the S11 function represents the resonance frequency. The resonance frequency is nearly constant until the S11 value is coupled to about −0.2 dB. However, when the S11 value is more coupled, the range of variation in frequency is large. The coupling can be made weaker to reduce the change in frequency, however, the coupling of −0.2 dB results in a change of only 0.5 MHz with respect to the reference frequency. For weaker couplings, signal strength is too weak and not suitable for practical experiments. The insertion depth of the E-probe with an S11 value of −0.2 dB is the point where the end of the inner conductor of the E-probe is 0.1 mm from the jig surface.

The E-probe consists of an inner and an outer conductor made of annealed brass, and the material between the conductors is Teflon (Epsilon = 2.1), used in several wiring and electronic components owing to its low di-

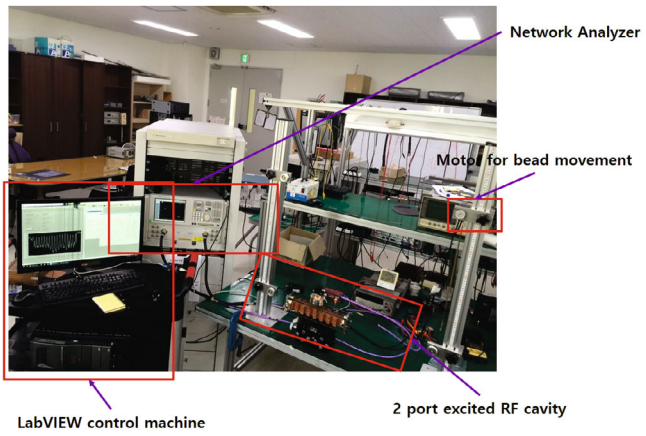

Fig. 6. (Color online) Ead-pull measurement system.

electric constant. The diameter of the inner conductor, outer conductor, and the axial gap distance between conductors are 0.5 mm, 2.5 mm, 0.75 mm, respectively. The resonance frequency of the RF cavity, assembled with the jig was simulated by CST Microwave Studio. The resonance frequencies of the normal and the side-coupled cells exhibit a frequency shift due to the presence of the short bar. The simulation results of the normal and side-coupled cells of the 7 bunching cells, the normal accelerating cell, a power coupler cell, and an end cell are listed in Table 2.

Figure 5 depicts measurement results of the resonance frequency of the differenct RF cavity cells. The results show that most of the fabricated RF cavity cells have an error of ±1 MHz with respect to the reference frequency, and such degree of frequency drift can be compensated by frequency tuning.

2. Bead-Pull Measurement

A. Fundamental theory of the bead-pull measurement

For a resonance condition in an RF cavity, the electric and magnetic field strengths are equal. However, when a small change in volume occurs in the wall of the RF cavity, or when a new material enters the RF cavity, which changes the magnetic or electric fields, the resonance frequency of the RF cavity changes. The resonant frequency variation of the RF cavity due to the external material can be explained using Eq. (3) of the Slater perturbation theorem, rewritten by Klein [13] in a more practical expression as:

$$\frac{\Delta\omega}{\omega} = -\frac{3\Delta V}{4U}\left(\epsilon E_0^2 - \frac{\mu H_0^2}{2}\right). \tag{3}$$

The bead-pull measurement system is a device determining the relative intensity of the electric field generated inside the RF cavity by measuring the magnitude of

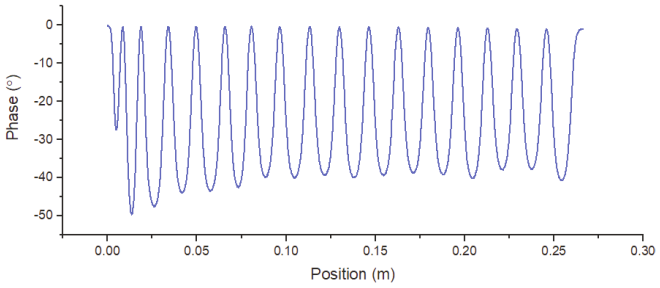

Fig. 7. (Color online) Electric field distribution in the RF cavity measured by the bead-pull measurement technique.

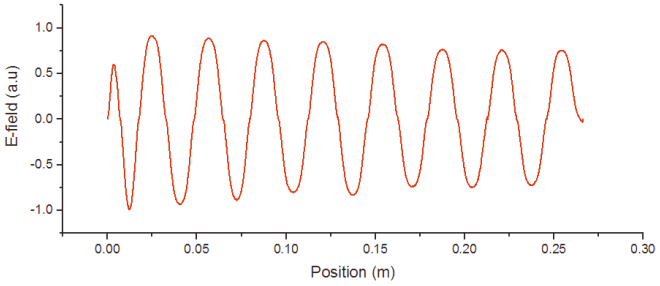

Fig. 8. (Color online) Converted electric field of the RF cavity.

change in the resonant frequency while the bead moves through the RF cavity [14]. However, for an RF cavity using an X-band range, the size of the RF cavity is small owing to the high frequency, thus a small-sized bead is required. If the bead size is small, the change measured in the frequency is very small, which is difficult to measure because of the high noise and long measurement time. Ma [15] showed that the resonance frequency change can be represented by the phase change of S21. Therefore, instead of the direct measurement of the resonance frequency change, it is possible to measure the electric field change with less noise by using the phase change. The experimental setup for the bead-pull measurement is shown in Fig. 6.

The frequency change due to the change in the phase of S21 can be expressed as follows [16,17]:

$$\Delta ang(\mathrm{S21}) = \tan^{-1}\left(\frac{-\Omega(f)}{1+\beta_1+\beta_2}\right) \tag{4}$$

with $\Omega(f) = Q_0\left(\frac{f}{f_0} - \frac{f_0}{f}\right)$, where f is the perturbed frequency, f_0 is the unperturbed frequency, Q_0 is the unloaded quality factor, and β_1 and β_2 are coupling coefficient for each probe.

The measured electric field distribution in the RF cavity by the bead-pull measurement technique is shown in Fig. 7. As the value measured by the bead-pull measurement is proportional to the square of the electric field, the square root is obtained and converted to a sinusoidal form. The electric field converted to a sinusoidal form is shown in Fig. 8. The results, obtained by using the AS-

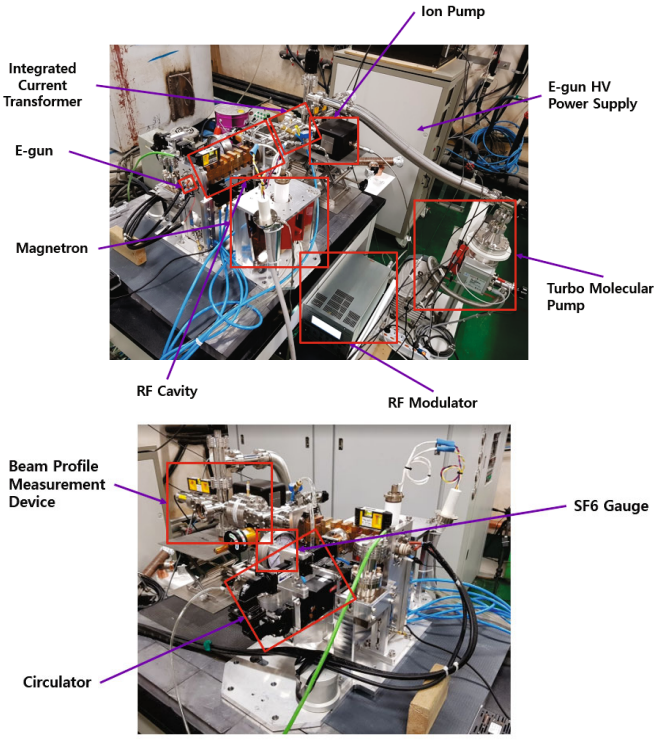

Fig. 9. (Color online) RF system for the 6 MeV X-band electron linac.

TRA simulation software with actual measured electric field data, confirmed that, compared to the ideal electric field, a power $\sim 3\%$ higher is required. During the design process of a 6 MeV electron linac for a dual-head gantry radiotherapy machine, the input power is designed to be 20% of the normal input power; therefore, a 3% increase in the input power is in a safe range.

IV. HIGH-POWER TEST AND BEAM MEASUREMENT

After the RF cavity resonance frequency and electric field map tuning were completed, an RF driving test was performed, where a magnetron was used to transmit the RF power to the RF cavity. Electrons generated in the cathode inside the magnetron were accelerated by the electric field, and the accelerated electrons were rotated by the magnetic field in the axial direction. The rotating electrons were coupled to the RF cavity placed on the outside, and the RF cavity excited by the wake field of the electrons emit the RF power to the outside by a power coupler. Therefore, a current source, to heat the filament of the thermal cathode and a high-voltage power supply, to generate the electric field between the cathode and the anode to accelerate the electrons, were required to drive the magnetron. The device, equipped with a control system to operate the magnetron, is known as

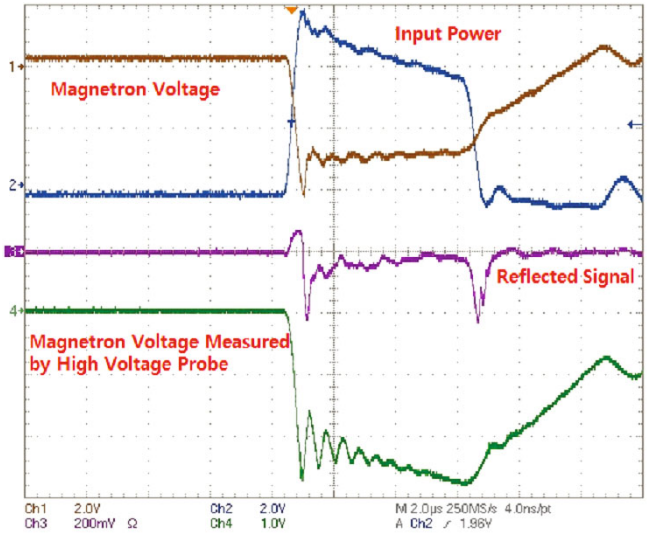

Fig. 10. (Color online) Magnetron signal measured by oscilloscope.

the RF modulator. In this study, a modulator manufactured by ScandiNova was used. The power generated by the magnetron is transmitted through the waveguide to the RF cavity. The type WR-112 waveguide employed in the X-band range was used in this study, which was able to withstand a peak power of 2 MW. To prevent arcing in the waveguide, the inside was filled with sulfur hexafluoride (SF_6)gas.

The RF cavity is designed and manufactured to receive all the RF power, generated by the magnetron during operation without reflection. However, as the maximum power is reflected instantly during the first switch-on, the magnetron should be protected by the reflected wave. Reflection of the RF power is further possible due to changes in the fine frequency and coupling state of the RF cavity, due to the unstable temperature and humidity during operation. A circulator was used to protect the magnetron from the wave reflected from the RF cavity.

The circulator directs the signal traveling toward the RF cavity direction and the signal coming from the opposite direction to a dummy load. The circulator used in the study was chosen to withstand a peak RF power of 2 MW and an average RF power of 3 kW. The construction of the test bench of the 6 MeV X-band electron linac for the dual-head gantry radiotherapy is shown in Fig. 9.

The high-power test of the electron linac was carried out at a temperature of 40 °C. The operating temperature range of the magnetron was 10 - 60 °C, and the operating temperature of the RF modulator was 10 - 40 °C. If the operating temperature is lower than room temperature, condensation occurs on the surface of the accelerator tube. Moreover, if the accelerator is operated at too high a temperature, turbulence occurs in the cooling line because the boiling water is used as cooling water, resulting in a rapid drop of the cooling efficiency,

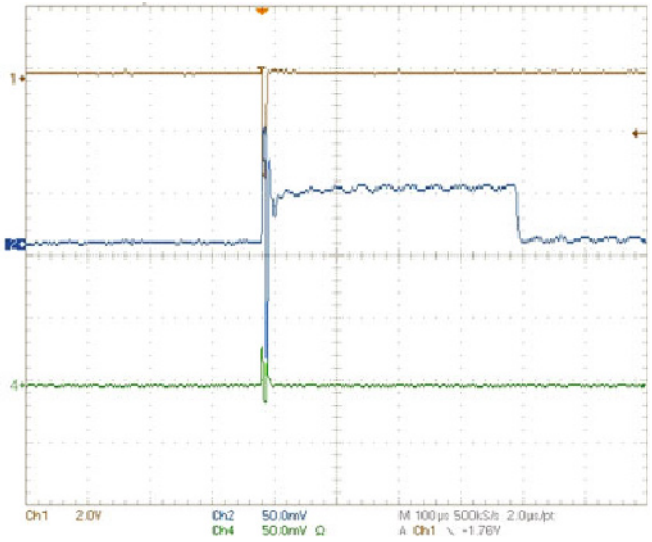

Fig. 11. (Color online) Results from the integrated current transformer.

thus high-temperature operation must be avoided. In addition, the RF cavity needs be operated at a temperature as low a as possible, because the electrical conductivity decreases with the increasing temperature. The design and testing of the RF cavity was performed at a 20 °C room temperature, however the actual operation was at 40 °C. As the measured resonance frequency of the RF cavity changes at a rate of −150 kHz/°C, it is tuned to 9.303 GHz, and to 9.3 GHz for the operation at 40 °C. The measured S11 value at 9.303 GHz was −29.811, and 0.1% of the input power will be reflected at the RF cavity.

Before the RF power was applied to the RF cavity for the first time, the RF cavity was baked at 300 °C, while the vacuum pump was operated simultaneously to remove oxygen compounds and impurities remaining on the inside copper surface of the RF cavity. After the baking is finished, an RF conditioning is required to put the RF power into the RF cavity. The RF power was applied to the inside of the RF cavity for a long period, with a power lower than the actual target power, to remove the impurities and the unstable parts. After completing the RF conditioning operation, the forward power was gradually increased, with simultaneously observing the reflected power strength during the high-power test. If electrical breakdown occurs, the reflected power increases sharply, and the vacuum of the RF cavity instantaneously deteriorates.

The forward and reflected power results with incident RF power are shown in Fig. 10. Using the high voltage generated by the modulator, it was confirmed that the RF output was properly generated when the operating voltage of the magnetron was reached. In Fig. 10, the yellow signal waveform represents the magnetron or modulator high voltage signal, the blue signal waveform represents the transmitted RF power signal, and the red

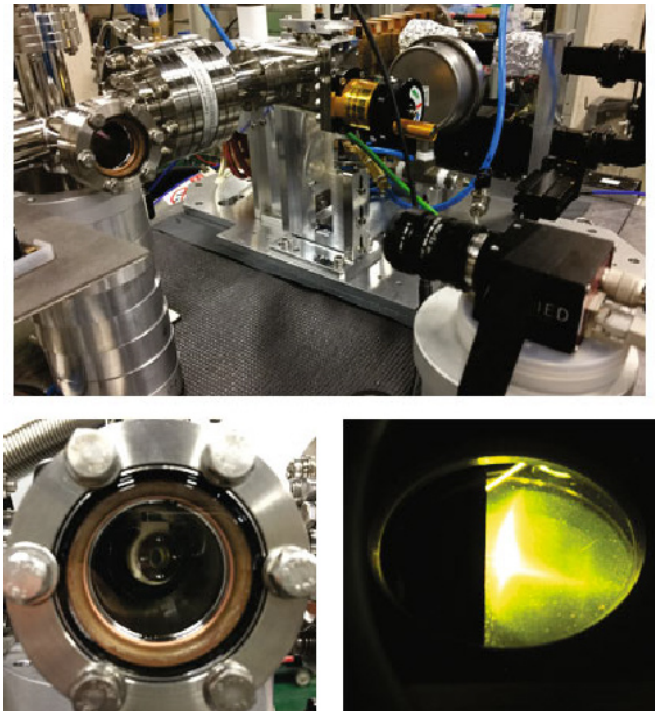

Fig. 12. (Color online) Beam profile measurement system using YAG screen and CCD camera.

signal waveform represents the reflected RF power signal. As can be seen in Fig. 10, it was confirmed that the RF power was properly fed without time delay when the applied modulator voltage signal was generated. Furthermore, it was confirmed that stable RF operation was achieved by adjusting the reflected wave to be minimal when the RF output generated was maximal.

After the high-power was injected into the RF cavity, the E-gun was powered up and the electron beam was induced to the accelerator. The current of the generated electron beam was measured indirectly through an integrated current transformer (ICT). The ICT-signal measured by the oscilloscope, shown in Fig. 11 is represented by the voltage, and the converted maximum beam current value is 16 mA for a duty factor of 0.008.

The electron beam profile and the electron beam current can be measured using an yttrium aluminum garnet (YAG) screen. The YAG screen is a type of scintillator, which emits fluorescent light when reacts with an electron beam. The apparatus for measuring the profile of the electron beam is shown in Fig. 12. When the YAG screen is hit by the electron beam, it emits light and its image is captured by a charge-coupled device (CCD) camera.

V. CONCLUSION

In this study, a 6 MeV electron linac for a dual-head gantry radiotherapy machine system was fabricated, and

verified. To operate the electron linac, acting as an X-ray generator to generate the specified 500 cG/min X-ray, an average beam current of 55 μA and an electron beam energy of 6 MeV is required. A specialized jig was designed to measure the resonance frequency of the fabricated RF cavity. For the frequency measurement, a position where sufficient signal can be obtained, even when the electric probe is inserted, was found, and the resonance frequencies of all RF cavity cells were measured and tuned to the desired frequency. To measure the electric field distribution inside the assembled RF cavity, a bead-pull measurement method based on perturbation theorem was used. The fabricated and tested RF cavity was assembled into an RF station, and RF conditioning and beam commissioning processes were performed.

ACKNOWLEDGMENTS

This work was supported by Institute for Information & communications Technology Promotion (IITP) grant funded by the Korea government (MSIP) (No. R0101-16-0126(10043897), Development of 500 cGy level radiation therapy system based on automatic detection and tracing technology with dual-head gantry for 30% reducing treatment time for cancel tumors) and Radiation Technology R&D program through the National Research Foundation of Korea funded by the Ministry of Science, ICT & Future Planning (2017M2A2A4A02020284).

REFERENCES

[1] T. R. Mackie, Phys. Med. Biol. **51**, R427 (2006), doi:10.1088/0031-9155/51/13/R24.

[2] Y. B. Kim and C. O. Suh, *Evolution of Radiotherapy: High precision Radiotherapy* (2008), p. 604.

[3] S. H. Lee *et al.*, Nucl. Instruments Methods Phys. Res. Sect. A Accel. Spectrometers, Detect. Assoc. Equip. **852**, 40 (2017), doi:10.1016/j.nima.2016.11.034.

[4] Accuray Inc., (n.d.), www.accuray.com.

[5] Y. Kamino, S. Miura, M. Kokubo, I. Yamashita, E. Hirai, M. Hiraoka and J. Ishikawa, Med. Phys. **34**, 1797 (2007), doi:10.1118/1.2723878.

[6] J. R. J. Adler, S. D. Chang, M. J. Murphy, J. Doty, P. Geis and S. L. Hancock, Stereotact. Funct. Neurosurg. **69**, 124 (1997).

[7] S. Hanna, *Applications of X-band technology in medical accelerators, Proc. 1999 Part. Accel. Conf.* (1999), p. 2516, doi:10.1109/PAC.1999.792751.

[8] J. W. Wang, *RF Properties Structures of Periodic for Linear Accelerating Colliders* (1989).

[9] V. Dolgashev, *High gradient, X-band and above, metallic RF structures* (2015).

[10] A. Tropp, *Studies of vacuum discharges in the CLIC accelerating structure* (Lund University, 2016).

[11] S-W. Shin *et al.*, J. Korean Phys. Soc. **71**, 1048 (2017), doi:10.3938/jkps.71.1048.

[12] J. C. Slater, Phys. Today. **3**, 3 (1950), doi:10.1063/1.3066836.

[13] H. Klein, Cern 92-03 **1**, 112 (1992).

[14] P. Schmuser, *Tuning of Multi-Cell Cavities using Bead Pull Measurements* (1992).

[15] Z. Ma, *RF properties of high-temperature superconducting materials* (Stanford University, 1995), https://search.proquest.com/docview/304219227?accountid=11840.

[16] S. Ghosh, A. Mandal, S. Seth and S. S. Som, Conf. Proc. **C110904**, 280 (2011).

[17] P. J. Petersan and S. M. Anlage, J. Appl. Phys. **84**, 3392 (1998), doi:10.1063/1.368498.